

Chapter 15

Numerical study of the high-contrast Stokes equation and its robust preconditioning

Burak Aksoylu and Zuhul Unlu

Abstract We numerically study the Stokes equation with high-contrast viscosity coefficients. The high contrast viscosity values create complications in the convergence of the underlying solver methods. To address this complication, we construct a preconditioner that is robust with respect to contrast size and mesh size simultaneously based on the preconditioner proposed by Aksoylu et al. (2008, *Comput. Vis. Sci.* 11, pp. 319–331). We examine the performance of our preconditioner against multigrid and provide a comparative study reflecting the effect of the underlying discretization and the aspect ratio of the mesh by utilizing the preconditioned inexact Uzawa and Minres solvers. Our preconditioner turns out to be most effective when used as a preconditioner to the inexact p-Uzawa solver and we observe contrast size and mesh size robustness simultaneously. As the contrast size grows asymptotically, we numerically demonstrate that the inexact p-Uzawa solver converges to the exact one. We also observe that our preconditioner is contrast size and mesh size robust under p-Minres when the Schur complement solve is accurate enough. In this case, the multigrid preconditioner loses both contrast size and mesh size robustness.

15.1 Introduction

The Stokes equation plays a fundamental role in the modeling of several problems in emerging geodynamics applications. Numerical solutions to the Stokes flow prob-

Burak Aksoylu (✉)

(a) Department of Mathematics, TOBB University of Economics and Technology, Ankara, 06560, Turkey;

(b) Department of Mathematics, Louisiana State University, Baton Rouge, LA 70803, USA, e-mail: baksoylu@etu.edu.tr

Zuhul Unlu

Department of Mathematics, Louisiana State University, Baton Rouge, LA 70803, USA, e-mail: zyeter1@math.lsu.edu

lems especially with high-contrast variations in viscosity is critically needed in the computational geodynamics community; see recent studies [26, 27, 34, 44]. The high-contrast viscosity corresponds to a small Reynolds number regime because the Reynolds number is inversely proportional to the viscosity value. One of the main applications of the high-contrast Stokes equation is the study of earth's mantle dynamics. The processes such as the long time scale dynamics of the earth's convecting mantle, the formation and subsequent evolution of plate tectonics can be satisfactorily modeled by the Stokes equation; see [26, 34, 35] for further details. Realistic simulation of mantle convection critically relies on the treatment of the two essential components of simulation: *the contrast size in viscosity* and *the mesh resolution*. Hence, our aim is to achieve robustness of the underlying preconditioner with respect to the contrast size and the mesh size simultaneously, which we call as *m*- and *h*-robustness, respectively.

Roughness of PDE coefficients causes loss of robustness of preconditioners. In [3, 4] Aksoylu and Beyer have studied the diffusion equation with such coefficients in the operator theory framework and have showed that the roughness of coefficients creates serious complications. For instance, in [4] they have shown that the standard elliptic regularity in the smooth coefficient case fails to hold. Moreover, the domain of the diffusion operator heavily depends on the regularity of the coefficients. Similar complications also arise in the Stokes case. This article came about from a need to address solver complications through the help of robust preconditioning. For that, we construct a robust preconditioner based on the one proposed in [2], which we call as the Aksoylu-Graham-Klie-Scheichl (AGKS) preconditioner. The AGKS preconditioner originates from the family of robust preconditioners constructed in [5]. It was proven and numerically verified to be *m*- and *h*-robust simultaneously.

The AGKS preconditioner was originally designed for the high-contrast diffusion equation under finite element discretization. In [6] we extended the AGKS preconditioner from finite element discretization to cell-centered finite volume discretization. Hence, we have shown that the same preconditioner could be used for different discretizations with minimal modification. Furthermore, in [7] we applied the same family of preconditioners to high-contrast biharmonic plate equation. Therefore, we have accomplished a desirable preconditioning design goal by using the same family of preconditioners to solve the elliptic family of PDEs with varying discretizations. In this article, we aim to bring the same preconditioning technology to *vector valued* problems such as the Stokes equation. We extend the usage of AGKS preconditioner to the solution of the stationary Stokes equation in a domain $\Omega \subset \mathbb{R}^2$:

$$\begin{aligned} -\nabla \cdot (v \nabla u) + \nabla p &= f & \text{in } \Omega, \\ \nabla \cdot u &= 0 & \text{in } \Omega, \end{aligned} \quad (15.1)$$

with piecewise constant high-contrast viscosity used in the slab subduction referred as the *Sinker* model by [34]:

$$v(x) = \begin{cases} m \gg 1, & x \in \Omega_H, \\ 1, & x \in \Omega_L. \end{cases} \quad (15.2)$$

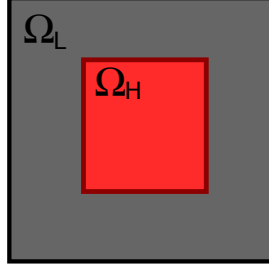


Fig. 15.1: $\Omega = \overline{\Omega_H} \cup \Omega_L$ where Ω_H and Ω_L are highly- and lowly-viscous regions, respectively.

Here, u , p , and f stand for the velocity, pressure, and body force, respectively.

The discretization of (15.1) gives rise to the following saddle point matrix:

$$\mathcal{A} \begin{bmatrix} u \\ p \end{bmatrix} = \begin{bmatrix} K(m) & B^t \\ B & 0 \end{bmatrix} \begin{bmatrix} u \\ p \end{bmatrix} = \begin{bmatrix} f \\ 0 \end{bmatrix}. \quad (15.3)$$

The velocity vector can be treated componentwise which allows the usage of a single finite element space for each component. The extension of AGKS preconditioner from diffusion to Stokes equation is accomplished by the following crucial block partitioning of (15.3); see [20, p. 226]:

$$\begin{bmatrix} K^x(m) & 0 & (B^x)^t \\ 0 & K^y(m) & (B^y)^t \\ B^x & B^y & 0 \end{bmatrix} \begin{bmatrix} u^x \\ u^y \\ p \end{bmatrix} = \begin{bmatrix} f^x \\ f^y \\ 0 \end{bmatrix}, \quad (15.4)$$

where $K^* = K^x = K^y$ are the scalar diffusion matrices, and B^x and B^y represent the weak derivatives in x and y directions, respectively. We apply the AGKS preconditioning idea to the K^x and K^y blocks by further decomposing each of them as the following 2×2 block system; see [7, Eqn. 11], [6, Eqn. 4], [2, Eqn. 3]:

$$K^*(m) = \begin{bmatrix} K_{HH}^*(m) & K_{HL}^* \\ K_{LH}^* & K_{LL}^* \end{bmatrix}, \quad (15.5)$$

where the degrees of freedom (DOF) are identified as *high* and *low* based on the viscosity value in (15.2) and K_{HH}^* , K_{HL}^* , K_{LH}^* , and K_{LL}^* denote couplings between the high-high, high-low, low-high, and low-low DOF, respectively. The exact inverse of K^* can be written as:

$$K^{*-1} = \begin{bmatrix} I_{HH} & -K_{HH}^{*-1} K_{HL}^* \\ 0 & I_{LL} \end{bmatrix} \begin{bmatrix} K_{HH}^{*-1} & 0 \\ 0 & S^{*-1} \end{bmatrix} \begin{bmatrix} I_{HH} & 0 \\ -K_{LH}^* K_{HH}^{*-1} & I_{LL} \end{bmatrix},$$

where I_{HH} and I_{LL} denote the identity matrices of the appropriate dimension and the Schur complement S^* is explicitly given by:

$$S^*(m) = K_{LL}^* - K_{LH}^* K_{HH}^{*-1}(m) K_{HL}^*. \quad (15.6)$$

The AGKS preconditioner is defined as follows:

$$\hat{K}^{*-1}(m) := \begin{bmatrix} I_{HH} & -K_{HH}^{\infty\dagger} K_{HL}^* \\ 0 & I_{LL} \end{bmatrix} \begin{bmatrix} K_{HH}(m)^{*-1} & 0 \\ 0 & S^{\infty-1} \end{bmatrix} \begin{bmatrix} I_{HH} & 0 \\ -K_{LH}^* K_{HH}^{\infty\dagger} & I_{LL} \end{bmatrix}, \quad (15.7)$$

where $K_{HH}^{\infty\dagger}$ and S^{∞} are the asymptotic values of K_{HH}^{*-1} and S^* , respectively; see [2, Lemma 1].

15.1.1 Literature Review

There are many solution methods proposed for the system of equations in (15.3); see the excellent survey article [13]. Based on where the emphasis is put in the design of a solution method, solving a saddle-point matrix system can be classified into two approaches: *preconditioning and solver*. The *preconditioning approach* aims to construct novel preconditioners for standard solver methods such as Uzawa and Minres. A vast majority of the articles on the *preconditioning* approach focuses on the preconditioning of Schur complement matrix; see [17, 31, 32, 34, 37, 39, 44]. It is well known that the Schur complement matrix S is spectrally equivalent to the pressure mass matrix (PMM) for the steady Stokes equation; see [16]. For rigorous convergence analysis of Krylov solvers with PMM preconditioner, see [42, 45]. Elman and Silvester [23] established that scaled PMM lead to h -robustness for the Stokes equation with large constant viscosity. Using a new inner product, Olshanskii and Reusken [37] introduced a robust preconditioner for the Schur complement matrix $S = BK^{-1}B'$ for discontinuous viscosity $0 < \nu \leq 1$ and showed that the preconditioned Uzawa (p-Uzawa) and Minres (p-Minres) became h -robust with this new PMM preconditioner. Further properties of this preconditioner such as clustering in the spectrum of preconditioned S system was shown in [29]. It was pointed out in [31] that Elman [18] designed LSQR commutator (BFBt) preconditioner in order to overcome the m -robustness issues by using $\hat{S} = (BB')^{-1}BKB'(BB')^{-1}$ preconditioner for S . This preconditioner is further studied in [17, 19]. Additionally, the usage of variants of the BFBt preconditioner for the high-contrast Stokes equation is popularized with $\nu|_{\Omega_H} = m \gg 1$ in geodynamics applications in [26, 27, 34, 44]. May and Moresi [34] established that this preconditioner was m -robust when used along with a preconditioned Schur Complement Reduction solver and h -robustness of this preconditioner when used with the Schur method and generalized conjugate residual method with block triangular preconditioners was obtained by a further study in [44].

There have been studies focusing on different ways of preconditioning K for the Stokes equation restricted to constant viscosity case; see [15, 22, 43]. It was observed that a single multigrid (MG) cycle with an appropriate smoother was usually a good preconditioner for K because MG is sufficiently effective as a preconditioner

for the constant viscosity case; see [20]. For discontinuous coefficient case, however, there has not been much study to analyze the performance of preconditioners for K in a Stokes solver framework. Since MG loses h -robustness, there is an imminent need for the robustness study of preconditioners for the case of discontinuous coefficients and we present the AGKS preconditioner to address this need.

The *solver method approach* aims to construct a solver by sticking with standard preconditioners such as MG for the K matrix and PMM or BFBt for the S matrix. The performance of the solver depends heavily on the choice of the inner preconditioner; see [9, 10, 22, 25]. The Uzawa solver is one of the most popular iterative methods for the saddle point problems in fluid dynamics; see [25, 28, 30]. Since this method requires the solution of K system in each step, this leads to the utilization of an inexact Uzawa method involving an approximate evaluation of K^{-1} ; see [11, 46]. This method involves an inner and outer iteration (in our context, S - and outer-solve, respectively), and the convergence of this method is studied extensively in [11, 15, 22, 39].

Another commonly used iterative method is Minres; see [38]. The usage of block diagonal preconditioner for the p-Minres solver was suggested in [24] and further results were presented for this type of preconditioning in [40]. For constant viscosity case, there have been many studies for different choices of the preconditioners for K and S blocks; see [13, 14, 39, 42, 45]. For the discontinuous viscosity case, on the other hand, Olshanskii and Reusken [36, 37] studied the performance of p-Minres with a new PMM preconditioner.

The remainder of the paper is structured as follows. In Section 15.2, we describe p-Uzawa and p-Minres solvers. In Section 15.3, we comparatively study the performance of the AGKS preconditioner against MG used under the above solvers. We highlight important aspects of robust preconditioning and draw some conclusions in Section 15.4.

15.2 Solver Methods

The LBB stability of Stokes discretizations has been extensively studied due to utilization of weak formulations to solve (15.1). We are interested in the LBB stability in the case of high-contrast coefficients. In [36], the LBB stability was proved only for the case $0 < \nu \leq 1$. Later, in [37] this restriction was eliminated and the results were extended to cover general viscosity, thereby, immediately establishing the LBB stability of the discretization under consideration as the following:

$$\sup_{u_h \in V_h} \frac{(\operatorname{div} u_h, p_h)}{\|u_h\|_V} \geq c_{LBB} \|p_h\|_Q, \quad p_h \in Q_h, \quad (15.8)$$

The associated spaces and weighted norms are defined as follows:

$$\begin{aligned}
V &:= [H_0^1(\Omega)]^d, \\
Q &:= \{p \in L^2(\Omega) : (v^{-1}p, 1) = 0\}, \\
\|u\|_V &:= (v\nabla u, \nabla v)^{\frac{1}{2}}, \quad u \in V, \\
\|p\|_Q &:= (v^{-1}p, p)^{\frac{1}{2}}, \quad p \in Q.
\end{aligned}$$

Here $V_h \subset V$ and $Q_h \subset Q$ are finite element spaces that are LBB stable. To be precise, we utilize the $Q2$ - $Q1$ (the so-called Taylor-Hood finite element) discretization for numerical experiments in Section 15.3.

There are many solution methods for the indefinite saddle point problem (15.3). We concentrate on two different solver methods: the p-Uzawa and p-Minres. We test the performance the AGKS preconditioner with these solver methods. First, we establish two spectral equivalences: between the velocity stiffness matrix K and the AGKS preconditioner and between the Schur complement matrix S and the scaled PMM. Note that the constant c_{LBB} in (15.8) is directly used for the spectral equivalence of S in the following.

Lemma 15.1. *Let \hat{K} and \hat{S} denote the AGKS preconditioner and the scaled PMM. Then, for sufficiently large m , the following spectral equivalences hold:*

$$(a) \quad (1 - cm^{-1/2})(\hat{K}u, u) \leq (Ku, u) \leq (1 + cm^{-1/2})(\hat{K}u, u), \quad (15.9)$$

for some constant c independent of m .

$$(b) \quad c_{LBB}^2(\hat{S}p, p)_Q \leq (Sp, p) \leq d(\hat{S}p, p)_Q, \quad (15.10)$$

where c_{LBB} is the constant in (15.8) which is independent of m and h .

Proof. One can extract a symmetric positive semidefinite matrix \mathcal{N}_{HH}^* with a rank one kernel from K_{HH}^* in (15.5). \mathcal{N}_{HH}^* is the so-called Neumann matrix and the extraction leads to the following decomposition:

$$K_{HH}^*(m) = m\mathcal{N}_{HH}^* + \Delta.$$

Δ corresponds to the coupling between the DOF in Ω_L and on the boundary of Ω_H . Since $\ker(\mathcal{N}_{HH}^*)$ has rank one, \mathcal{N}_{HH}^* has a simple zero eigenvalue and the below spectral decomposition holds with $\lambda_i > 0$, $i = 1, \dots, n_H - 1$ where n_H denotes the order of \mathcal{N}_{HH}^* :

$$Z^t \mathcal{N}_{HH}^* Z = \text{diag}(\lambda_1, \dots, \lambda_{n_H-1}, 0).$$

Although the eigenvectors in the columns of Z and the eigenvalues λ_i can change according to the underlying discretization, there is always one simple zero eigenvalue and its corresponding constant eigenvector independent of the discretization. This is a direct consequence of the diffusion operator corresponding to a Neumann problem. Therefore, the spectral equivalence established for the $P1$ finite element in [2, Thm. 1] extends to $Q2$ and $Q1$ discretizations, thereby, completing the proof of part (a) for K^* . The spectral equivalence of K easily follows from that of K^* because of the decomposition in (15.4).

The proof of (b) follows from [37, Thm. 6]. \square

15.2.1 The Preconditioned Uzawa Solver

The Uzawa algorithm is a classical solution method which involves block factorization with forward and backward substitution. Here, we use the preconditioned inexact Uzawa method described in [12] and [39]. The system (15.3) can be block factorized as follows:

$$\begin{bmatrix} K(m) & 0 \\ B & -I \end{bmatrix} \begin{bmatrix} I & K(m)^{-1}B^t \\ 0 & S(m) \end{bmatrix} \begin{bmatrix} u \\ p \end{bmatrix} = \begin{bmatrix} f \\ 0 \end{bmatrix}. \quad (15.11)$$

Let (u^k, p^k) be a given approximation of the solution (u, p) . Using the block factorization (15.11) combined with a preconditioned Richardson iteration, one obtains:

$$\begin{bmatrix} u^{k+1} \\ p^{k+1} \end{bmatrix} = \begin{bmatrix} u^k \\ p^k \end{bmatrix} + \begin{bmatrix} I & -K^{-1}B^tS^{-1} \\ 0 & S^{-1} \end{bmatrix} \begin{bmatrix} K^{-1} & 0 \\ BK^{-1} & -I \end{bmatrix} \left(\begin{bmatrix} f \\ 0 \end{bmatrix} - \mathcal{A} \begin{bmatrix} u^k \\ p^k \end{bmatrix} \right). \quad (15.12)$$

This leads to the following iterative method:

$$u^{k+1} = u^k + w^k - \hat{K}^{-1}B^t z^k, \quad (15.13a)$$

$$p^{k+1} = p^k + z^k, \quad (15.13b)$$

where $w^k := \hat{K}^{-1}r_1^k$, $r_1^k := f - Ku^k - B^t p^k$, and $z^k := \hat{S}B(w^k + u^k)$. Here, \hat{K} and \hat{S} are the AGKS and PMM preconditioners for K and S , respectively. Computing z^k involves ℓ iterations of pCG. In this computation, since the assembly of S is prohibitively expensive, first we replace it by \tilde{S} . Then, we utilize the preconditioner \hat{K} for K and \hat{S} for \tilde{S} where the explicit formula is given by:

$$\tilde{S} := B\hat{K}^{-1}B^t. \quad (15.14)$$

Thus, the total number of applications of \hat{K}^{-1} in (15.13a) and (15.13b) becomes $\ell + 2$. We refer the outer-solve (one Uzawa iteration) as steps (15.13a) and (15.13b) combined. In particular, we call the the computation of z^k as an S -solve; see Table 15.1. The stopping criterion of the S -solve plays an important for the efficiency of the Uzawa method and it is affected by the accuracy of \hat{K} ; see the analysis in [39, Sec. 4]. When the AGKS preconditioner is used for velocity stiffness matrix, the stopping criterion of the S -solve is determined as follows:

Let r_p^i be the residual of the S -solve at iteration i . Then, we abort the iteration when $\frac{\|r_p^i\|}{\|r_p^0\|} \leq \delta_{tol}$ where

- $\delta_{tol} = 0.5$ or
- maximum iteration reaches 4.

15.2.2 The Preconditioned Minres Solver

The p-Minres is a popular iterative method applied to the system (15.3). Let $v := \begin{bmatrix} u \\ p \end{bmatrix}$. With the given initial guess $v^0 := \begin{bmatrix} u^0 \\ p^0 \end{bmatrix}$ where $p^0 \in e^{\perp \varrho}$ and with the corresponding error $r^0 := v - v^0$, the p-Minres solver computes:

$$v^k = \underset{v \in v^0 + \mathcal{K}^k(\mathcal{B}^{-1}\mathcal{A}, r^0)}{\operatorname{argmin}} \left\| \mathcal{B}^{-1} \begin{bmatrix} f \\ 0 \end{bmatrix} - \mathcal{A} v \right\|.$$

Here, $\tilde{r}^0 = \mathcal{B}^{-1}r^0$ and $\mathcal{K}^k = \operatorname{span}\{\tilde{r}^0, \mathcal{B}^{-1}\mathcal{A}\tilde{r}^0, \dots, (\mathcal{B}^{-1}\mathcal{A})^k\tilde{r}^0\}$, and the preconditioner has the following block diagonal structure:

$$\mathcal{B} = \begin{bmatrix} \hat{K} & 0 \\ 0 & \hat{S} \end{bmatrix}, \quad (15.15)$$

where \hat{K} and \hat{S} are the preconditioners for K and S , respectively. In each step of the p-Minres solver the above preconditioner is applied in the following fashion: for the K -block one application of \hat{K} and for the S -block several applications of pCG to the \tilde{S} -system with \hat{S} as the preconditioner. Here, $\tilde{S} = B\hat{K}^{-1}B^t$ stands for the approximation of S . Since S is replaced by \tilde{S} , this turns the p-Minres algorithm to an inexact one; see the inexactness discussion in Section 15.3.2. The p-Minres iterations are called outer-solve whereas the pCG solve for the \tilde{S} -system is called inner-solve.

The convergence rate of the p-Minres method depends on the condition number of the preconditioned matrix, $\mathcal{B}^{-1}\mathcal{A}$. Combining the spectral equivalences given in (15.9) and (15.10) with the well-known condition number estimate [8], we obtain:

$$\kappa_{\mathcal{B}}(\mathcal{B}^{-1}\mathcal{A}) \leq \frac{\max\{(1 + cm^{-1/2}), d\}}{\min\{(1 - cm^{-1/2}), c_{LBB}^2\}}$$

It immediately follows that the convergence rate of the p-Minres method is independent of m asymptotically.

15.3 Numerical Experiments

The goal of the numerical experiments is to compare the performance of the AGKS and MG preconditioners by using two different solvers: p-Uzawa and p-Minres. We use a four-level hierarchy in which the numbers of DOF, N_1, N_2, N_3 , and N_4 , are 659, 2467, 9539, and 37507 from coarsest to finest level. We consider cavity flow with enclosed boundary conditions with right hand side functions $f = 1$ and $g = 0$ on a 2D domain $[-1, 1] \times [-1, 1]$.

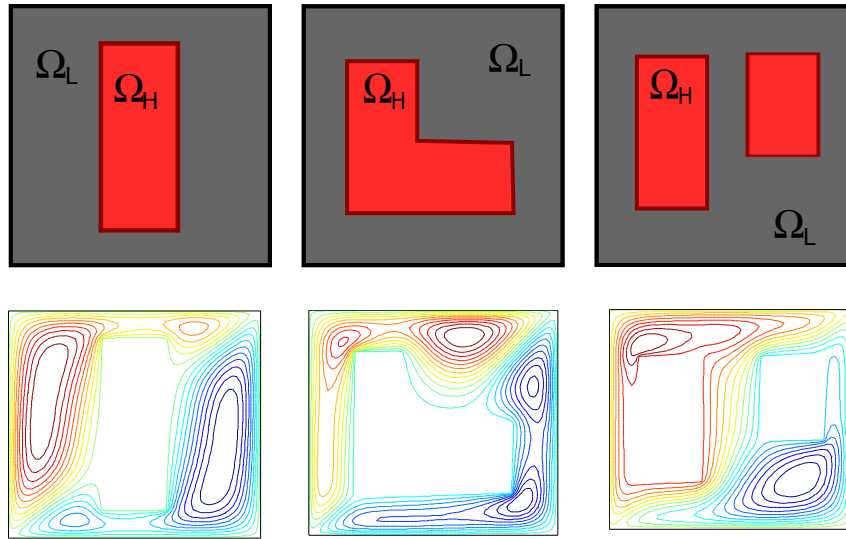


Fig. 15.2: The streamline plot of the high-contrast Stokes equation for three different high-viscosity island configurations; (left) rectangular, (middle) L-shaped, and (right) two disconnected islands.

For discretization, we use the Q_2-Q_1 (the Taylor-Hood) stable finite elements and stabilized Q_1-Q_1 finite elements for the velocity-pressure pair. We consider the case of a single island (viscous inclusion) located at the region $[-1/4, 1/4] \times [-3/4, 3/4]$. For an extension, we also consider the cases of L-shaped island and two disconnected islands; see Figure 15.2. The observation about these cases are given in Section 15.4. The implementation of discretization is based on ifiss3.1 software provided in [41]; also see [21]. The AGKS preconditioner implementation is based on our implementation in [2, 6, 7]. The implementation of the MG preconditioner is derived from the one in [1]. We employ a V(1,1)-cycle, with point Gauss-Seidel (GS) smoother. A direct solver is used for the coarsest level. For each level of refinement, we present the number of iteration and average reduction factor corresponding to each solve (outer-solve and S -solve; outer-solve and inner-solve for p-Uzawa and p-Minres iterations, respectively). In the tables, N stand for the number of DOF in \mathcal{A} for the outer-solves and the number of DOF in S for the S - and inner-solves. We enforce an iteration bound of 200. If the method seems to converge slightly beyond this bound, we denote it by *. A zero initial guess is used. The numerical experiments were performed on a dual core Macbook Pro, running at 2.4 GHz with 4GB RAM.

In analyzing m -robustness, we observe a special feature. The iteration count remains fixed when m becomes larger than a certain threshold value. We define the notion *asymptotic regime* to indicate m values bigger than this threshold. Identifying an asymptotic regime is desirable because it immediately indicates m -robustness.

Table 15.1: Number of iterations and average reduction factors for p-Uzawa, Q_2-Q_1 , rectangular mesh, MG.

$N \setminus m$	10^0	10^1	10^2	10^3	10^4	10^5	10^6	10^7	10^8	10^9
outer-solve										
659	13,0.546	15,0.594	15,0.517	17,0.517	19,0.506	19,0.596	19,0.589	19,0.588	22,0.588	22,0.589
2467	13,0.516	17,0.531	17,0.552	18,0.456	20,0.456	21,0.455	21,0.455	21,0.455	21,0.456	21,0.460
9539	18,0.345	20,0.460	20,0.487	23,0.491	25,0.492	26,0.491	27,0.683	28,0.677	31,0.678	32,0.698
37507	13,0.371	23,0.476	23,0.509	26,0.508	27,0.503	38,0.502	35,0.500	40,0.499	48,0.800	50,0.825
S-solve										
81	2,0.797	3,0.703	2,0.715	2,0.726	3,0.729	3,0.729	3,0.729	3,0.729	2,0.729	2,0.729
289	4,0.899	4,0.903	4,0.912	4,0.915	4,0.915	4,0.915	4,0.915	4,0.915	4,0.915	4,0.915
1089	1,0.997	2,0.802	3,0.914	4,0.919	4,0.920	4,0.920	4,0.920	3,0.920	3,0.920	3,0.920
4225	1,0.995	1,0.800	1,0.913	1,0.920	3,0.920	2,0.921	4,0.981	3,0.921	4,0.941	3,0.921

Table 15.2: Number of iterations and average reduction factors for p-Uzawa, Q_2-Q_1 , rectangular mesh, AGKS.

$N \setminus m$	10^0	10^1	10^2	10^3	10^4	10^5	10^6	10^7	10^8	10^9
outer-solve										
659	24,0.546	15,0.394	14,0.417	14,0.417	14,0.406	14,0.396	14,0.389	14,0.388	14,0.388	14,0.389
2467	38,0.316	21,0.431	18,0.452	19,0.456	18,0.456	18,0.455	18,0.455	18,0.455	18,0.456	18,0.460
9539	47,0.745	31,0.660	16,0.487	16,0.491	15,0.492	15,0.491	15,0.483	15,0.477	15,0.478	15,0.480
37507	70,0.871	50,0.476	17,0.509	16,0.508	15,0.503	15,0.502	15,0.500	15,0.499	15,0.500	15,0.501
S-solve										
81	3,0.420	2,0.495	3,0.420	3,0.427	3,0.408	3,0.403	3,0.401	3,0.403	3,0.403	3,0.403
289	3,0.420	3,0.495	3,0.420	3,0.427	3,0.408	3,0.403	3,0.401	3,0.403	3,0.403	3,0.403
1089	1,0.620	1,0.695	3,0.620	1,0.627	1,0.608	1,0.603	1,0.601	1,0.603	1,0.603	1,0.603
4225	1,0.620	1,0.695	3,0.620	1,0.627	1,0.608	1,0.603	1,0.601	1,0.603	1,0.603	1,0.603

15.3.1 The Preconditioned Uzawa Solver

We use pCG solver with scaled PMM as a preconditioner, 0.5 as tolerance and 4 as maximum number of iterations, for the S -system in each iteration of p-Uzawa. The tolerance for the outer-solve is set to be 5×10^{-6} . We report the performance of the p-Uzawa solver applied to a rectangular and skewed mesh with Q_2-Q_1 discretization. We observe that the p-Uzawa method is m -robust as long as the optimal stopping criterion is used for the S -solve; see Tables 15.1- 15.6. The performances of the AGKS and MG preconditioners are observed as follows. When the MG preconditioner is used, the p-Uzawa solver loses m - and h -robustness and the iteration count increases dramatically when the mesh aspect ratio or the island configuration changes; see Tables 15.1, 15.3, and 15.5. Especially for viscosity values larger than 10^5 , we further observe that the iteration number of pCG method for the S -solve, denoted by ℓ , reaches the maximum iteration count 4. Since the MG preconditioner is applied $\ell + 2$ times at each iteration of the outer solve, we illustrate how this results in an unreasonable number of applications of the MG preconditioner; see Figure 15.3. For instance in Table 15.1, for the case of $m = 10^8$, we have $\ell = 4$. Therefore, in each outer-iteration, we apply the MG preconditioner $\ell + 2 = 6$ times. At level = 4, since the total number of MG application is the product of the outer-solve count with $\ell + 2$, it becomes $48 \times 6 = 288$. The iteration increases even more rapidly as we refine the mesh. Therefore, the loss of h -robustness sets a major drawback as larger size problems are considered.

Table 15.3: Number of iterations and average reduction factors for p-Uzawa, Q_2-Q_1 , skewed mesh, MG.

$N \setminus m$	10^0	10^1	10^2	10^3	10^4	10^5	10^6	10^7	10^8	10^9
outer-solve										
659	16 ,0.477	18 ,0.488	70 ,0.817	*,0.977	*,0.996	*,0.996	*,0.989	*,0.988	*,0.988	*,0.989
2467	18 ,0.616	21 ,0.631	24 ,0.652	34 ,0.706	80 ,0.856	*,0.955	*,0.955	*,0.965	*,0.956	*,0.990
9539	19 ,0.515	23 ,0.570	32 ,0.687	*,0.991	*,0.952	*,0.991	*,0.983	*,0.687	*,0.978	*,0.998
37507	17 ,0.471	27 ,0.576	27 ,0.569	72 ,0.808	97 ,0.883	*,0.962	*,0.990	*,0.999	*,0.980	*,0.985
S -solve										
81	2 ,0.797	3 ,0.703	2 ,0.715	2 ,0.726	3 ,0.729	3 ,0.729	3 ,0.729	3 ,0.729	3 ,0.729	3 ,0.729
289	4 ,0.899	4 ,0.903	4 ,0.912	4 ,0.915	4 ,0.915	3 ,0.915	4 ,0.915	4 ,0.915	4 ,0.915	4 ,0.915
1089	1 ,0.997	2 ,0.802	3 ,0.914	4 ,0.919	4 ,0.920	3 ,0.920	4 ,0.920	3 ,0.920	3 ,0.920	3 ,0.920
4225	2 ,0.995	1 ,0.800	1 ,0.913	2 ,0.920	3 ,0.920	3 ,0.921	4 ,0.981	3 ,0.921	3 ,0.941	3 ,0.921

Table 15.4: Number of iterations and average reduction factors for p-Uzawa, $Q2-Q1$, skewed mesh, AGKS.

$N \setminus m$	10^0	10^1	10^2	10^3	10^4	10^5	10^6	10^7	10^8	10^9
outer-solve										
659	33 ,0.695	23 ,0.580	21 ,0.556	21 ,0.553	22 ,0.564	22 ,0.564	22 ,0.564	21 ,0.545	19 ,0.529	25 ,0.603
2467	57 ,0.805	29 ,0.649	23 ,0.592	27 ,0.632	29 ,0.653	33 ,0.684	35 ,0.700	24 ,0.639	32 ,0.720	33 ,0.693
9539	72 ,0.875	39 ,0.733	31 ,0.666	38 ,0.728	32 ,0.682	40 ,0.737	33 ,0.691	31 ,0.667	31 ,0.701	31 ,0.708
37507	91 ,0.921	59 ,0.811	31 ,0.679	36 ,0.708	28 ,0.633	32 ,0.762	30 ,0.700	29 ,0.669	31 ,0.698	31 ,0.701
S -solve										
81	2 ,0.750	2 ,0.722	2 ,0.769	2 ,0.806	2 ,0.915	2 ,0.918	2 ,0.918	2 ,0.922	5 ,0.897	5 ,0.916
289	3 ,0.814	3 ,0.791	2 ,0.800	3 ,0.727	3 ,0.708	3 ,0.703	4 ,0.711	3 ,0.723	2 ,0.703	3 ,0.703
1089	2 ,0.700	3 ,0.695	3 ,0.720	2 ,0.727	2 ,0.708	2 ,0.688	2 ,0.701	2 ,0.713	2 ,0.693	2 ,0.703
4225	3 ,0.720	2 ,0.695	3 ,0.720	2 ,0.697	2 ,0.688	2 ,0.603	2 ,0.701	2 ,0.703	2 ,0.723	2 ,0.713

On the other hand, the AGKS preconditioner maintains m - and h -robustness simultaneously. Asymptotically, only one iteration of pCG is sufficient to obtain an accurate S -solve for a rectangular mesh; see Table 15.2. When we do the above calculation, we find that for a rectangular mesh, the total number of AGKS applications is $15 \times (1 + 2) = 45$. Since this application count remains fixed as the mesh is refined, we infer the h -robustness of the AGKS preconditioner; see Figure 15.3. When the mesh aspect ratio or the island configuration changes, number of pCG iterations required to have an accurate S -solve becomes 2 or 3. However, this is reasonable since the outer-solve maintains h - an m - robustness; see Tables 15.4, and 15.6. Hence, the AGKS preconditioner will acceleratedly outperform the MG preconditioner as more mesh refinements are introduced regardless of the island or mesh configuration.

15.3.2 The Preconditioned Minres Solver

We notice that the p-Minres has not been the solver of choice for high-contrast problems due to its unfavorable performance with PMM for the S -system; see [36]. We have taken a novel approach for the S system. First, we replace S by $\tilde{S} = B\hat{K}^{-1}B^t$ where \hat{K}^{-1} step is one application of the AGKS preconditioner. This makes the solver method *inexact*. Then, we solve \tilde{S} system by using a pCG solver with scaled PMM preconditioner with tolerance 0.05 with a maximum of 20 iterations. The pCG and p-Minres solution steps are called the inner- and outer-solve, respectively.

Table 15.5: Number of iterations and average reduction factors for p-Uzawa, Q_2-Q_1 , rectangular mesh, L-shaped island, MG.

$N \setminus m$	10^0	10^1	10^2	10^3	10^4	10^5	10^6	10^7	10^8	10^9
outer-solve										
659	12,0.377	16,0.478	27,0.617	67,0.717	97,0.817	*,0.976	*,0.969	*,0.980	*,0.988	*,0.989
2467	13,0.316	17,0.431	17,0.452	20,0.546	80,0.836	*,0.951	*,0.965	*,0.962	*,0.976	*,0.992
9539	18,0.525	24,0.575	25,0.607	29,0.657	87,0.887	*,0.981	*,0.978	*,0.987	*,0.988	*,0.998
37507	18,0.491	27,0.667	27,0.649	49,0.778	50,0.793	*,0.962	*,0.995	*,0.993	*,0.998	*,0.985
S -solve										
81	2,0.797	3,0.703	2,0.715	2,0.726	3,0.729	3,0.729	3,0.729	3,0.729	3,0.729	3,0.729
289	4,0.899	4,0.903	4,0.912	4,0.915	4,0.915	3,0.915	4,0.915	4,0.915	4,0.915	4,0.915
1089	1,0.997	2,0.802	3,0.914	4,0.919	4,0.920	3,0.920	4,0.920	3,0.920	3,0.920	3,0.920
4225	2,0.995	1,0.800	1,0.913	2,0.920	3,0.920	3,0.921	4,0.981	3,0.921	3,0.941	3,0.921

Our approach for the S -system is similar to the one we take in the p-Uzawa solver. But, notice that now the inner solver requires more accuracy in order to guarantee a convergent p-Minres solver.

Table 15.6: Number of iterations and average reduction factors for p-Uzawa, Q_2-Q_1 , rectangular mesh, L-shaped island, AGKS.

$N \setminus m$	10^0	10^1	10^2	10^3	10^4	10^5	10^6	10^7	10^8	10^9
outer-solve										
659	30,0.660	23,0.583	22,0.568	23,0.580	24,0.596	26,0.616	25,0.611	27,0.628	25,0.613	25,0.609
2467	52,0.791	27,0.631	18,0.503	16,0.454	19,0.525	18,0.509	19,0.527	21,0.581	21,0.556	21,0.560
9539	68,0.875	50,0.780	24,0.591	22,0.591	23,0.582	28,0.611	28,0.653	29,0.687	31,0.687	32,0.718
37507	73,0.871	53,0.796	25,0.599	24,0.510	26,0.524	34,0.512	35,0.502	33,0.490	42,0.804	42,0.815
S -solve										
81	2,0.787	3,0.703	2,0.717	2,0.726	3,0.729	3,0.725	3,0.729	3,0.729	2,0.739	2,0.729
289	4,0.895	4,0.904	4,0.922	4,0.911	4,0.935	4,0.921	4,0.915	4,0.915	4,0.912	4,0.915
1089	2,0.997	3,0.802	3,0.914	3,0.921	4,0.920	4,0.920	4,0.919	3,0.920	3,0.920	3,0.920
4225	2,0.995	2,0.810	2,0.913	2,0.920	3,0.919	2,0.921	3,0.981	3,0.921	4,0.941	3,0.921

Table 15.7: Number of iterations and average reduction factors for p-Minres, Q_2-Q_1 , rectangular mesh, MG.

$N \setminus m$	10^0	10^1	10^2	10^3	10^4	10^5	10^6	10^7	10^8	10^9
outer-solve										
659	15,0.546	15,0.594	18,0.517	19,0.517	19,0.506	19,0.596	20,0.589	20,0.588	23,0.588	24,0.589
2467	20,0.516	19,0.531	21,0.552	24,0.456	23,0.456	24,0.455	25,0.455	28,0.455	29,0.456	30,0.460
9539	21,0.345	19,0.460	24,0.487	24,0.491	24,0.492	24,0.491	25,0.683	26,0.677	28,0.678	32,0.698
37507	21,0.371	21,0.476	23,0.509	26,0.508	30,0.503	26,0.502	29,0.500	31,0.499	34,0.800	36,0.825
inner-solve										
81	6,0.497	7,0.623	7,0.655	7,0.666	7,0.649	7,0.659	7,0.659	7,0.659	7,0.660	7,0.661
289	8,0.699	9,0.703	9,0.713	9,0.720	9,0.715	9,0.717	9,0.713	9,0.721	9,0.735	9,0.735
1089	9,0.747	11,0.752	11,0.744	11,0.749	11,0.750	11,0.760	11,0.759	11,0.761	11,0.762	11,0.760
4225	12,0.795	13,0.801	13,0.813	13,0.810	13,0.811	13,0.801	13,0.803	13,0.805	13,0.808	13,0.811

Table 15.8: Number of iterations and average reduction factors for p-Minres, Q_2-Q_1 , rectangular mesh, AGKS.

$N \setminus m$	10^0	10^1	10^2	10^3	10^4	10^5	10^6	10^7	10^8	10^9
outer-solve										
659	29,0.546	23,0.394	18,0.417	16,0.417	18,0.406	16,0.396	16,0.389	18,0.388	20,0.388	20,0.389
2467	40,0.316	30,0.431	17,0.452	17,0.456	16,0.456	16,0.455	16,0.455	19,0.455	19,0.456	19,0.460
9539	50,0.745	45,0.660	20,0.487	20,0.491	19,0.492	16,0.491	16,0.483	20,0.477	20,0.478	20,0.608
37507	70,0.871	52,0.476	22,0.509	20,0.508	19,0.503	16,0.502	16,0.500	20,0.499	20,0.500	20,0.525
inner-solve										
81	20,0.797	20,0.703	5,0.585	5,0.576	5,0.579	5,0.529	5,0.569	5,0.548	5,0.567	5,0.554
289	20,0.763	20,0.694	5,0.580	5,0.572	5,0.582	5,0.532	5,0.556	5,0.552	5,0.571	5,0.548
1089	20,0.773	20,0.714	5,0.580	5,0.575	5,0.578	5,0.532	5,0.561	5,0.555	5,0.562	5,0.556
4225	20,0.768	20,0.701	5,0.583	5,0.573	5,0.576	5,0.530	5,0.561	5,0.550	5,0.548	5,0.552

As in the p-Uzawa case, the effectiveness of the AGKS preconditioner has been confirmed as it maintains both the m - and h -robustness whereas MG suffers from the loss of both; see Tables 15.7 - 15.12. Furthermore, we observe that the choice of \hat{K}^{-1} —an application of either MG or AGKS—in the inner-solve dramatically affects the performance inner-solve. Specifically, the scaled PMM preconditioner is m -robust, but not h -robust for the inner-solve with MG, whereas it is both m - and h -robust for inner-solve with AGKS regardless of the mesh aspect ratio or island configuration.

15.4 Conclusion

We provide several concluding remarks on the performance of the AGKS preconditioner under two different solvers. For p-Uzawa and p-Minres solvers, we report numerical results for only $Q2-Q1$ discretization on a rectangular or skewed mesh with a single square shaped or L-shaped island.

The p-Uzawa solver turns out to be the best choice since AGKS preserves both m - and h -robustness regardless of the discretization type or deterioration in the aspect ratio of the mesh. The change in one of the above only causes increase in the number of iterations, but qualitatively m - and h -robustness are maintained. Moreover, we observe that the asymptotic regime of the p-Uzawa solver starts with the m value 10^3 ; see left-bottom in Figure 15.3. As island configuration changes, the number of iterations of both K - and S -solve slightly increases. In addition to that, as the discretization changes, the m -robustness of PMM for S -solve is lost. The asymptotic regime of the p-Uzawa solver becomes $m \geq 10^7$; see Tables 15.4 and 15.6.

The AGKS preconditioner under the p-Minres solver also maintains both m - and h -robustness as the discretization, the aspect ratio of the mesh, or the island configuration change. However, the number of iterations in the p-Minres solver increases dramatically when the mesh is skewed. Compared to p-Uzawa, one needs a more accurate inner-solve for a convergent p-Minres. In addition, the asymptotic regime of p-Minres solver is $m \geq 10^7$. Combining these three features, p-Minres becomes less desirable compared to p-Uzawa; see bottom-right and top-right in Figure 15.3. However, this solver is potentially useful for large size problems as the AGKS preconditioner maintains h -robustness.

Acknowledgement

B. Aksoylu was supported in part by National Science Foundation DMS 1016190 grant and European Union Marie Curie Career Integration Grant 293978 grant.

Table 15.9: Number of iterations and average reduction factors for p-Minres, $Q2-Q1$, skewed mesh, MG.

$N \setminus m$	10^0	10^1	10^2	10^3	10^4	10^5	10^6	10^7	10^8	10^9
outer-solve										
659	18,0.547	19,0.578	19,0.582	28,0.657	43,0.767	88,0.897	*,0.999	*,0.999	*,0.998	*,0.999
2467	20,0.556	21,0.581	26,0.622	32,0.706	46,0.786	92,0.905	*,0.942	*,0.971	*,0.989	*,0.995
9539	20,0.545	25,0.578	29,0.677	43,0.757	57,0.817	97,0.917	*,0.978	*,0.987	*,0.988	*,0.998
37507	20,0.561	27,0.657	31,0.679	49,0.783	70,0.813	119,0.883	*,0.991	*,0.998	*,0.998	*,0.999
inner-solve										
81	6,0.499	9,0.633	9,0.675	9,0.686	9,0.679	9,0.679	9,0.679	9,0.679	9,0.680	9,0.681
289	8,0.729	10,0.753	10,0.753	10,0.760	10,0.755	10,0.757	10,0.753	10,0.761	10,0.775	10,0.775
1089	9,0.787	13,0.792	13,0.784	13,0.789	13,0.790	13,0.810	13,0.819	13,0.811	13,0.822	13,0.820
4225	12,0.825	15,0.851	15,0.865	15,0.860	15,0.861	15,0.851	15,0.853	15,0.855	15,0.858	15,0.861

Table 15.10: Number of iterations and average reduction factors for p-Minres, $Q2-Q1$, skewed mesh, AGKS.

$N \setminus m$	10^0	10^1	10^2	10^3	10^4	10^5	10^6	10^7	10^8	10^9
outer-solve										
659	33,0.694	26,0.647	26,0.644	27,0.649	27,0.654	29,0.663	29,0.665	31,0.679	39,0.753	38,0.785
2467	59,0.816	33,0.713	29,0.674	29,0.690	37,0.733	36,0.740	36,0.761	46,0.773	49,0.792	48,0.783
9539	75,0.875	44,0.772	34,0.702	34,0.711	49,0.782	58,0.814	60,0.820	60,0.840	70,0.893	72,0.902
37507	90,0.851	55,0.807	38,0.729	39,0.733	50,0.783	61,0.823	68,0.840	68,0.858	75,0.903	72,0.902
inner-solve										
81	25,0.817	23,0.813	15,0.787	15,0.776	15,0.779	15,0.729	15,0.769	15,0.748	15,0.767	15,0.754
289	20,0.763	20,0.694	15,0.780	15,0.772	15,0.782	15,0.732	15,0.776	15,0.772	15,0.771	15,0.748
1089	20,0.773	20,0.714	15,0.780	15,0.777	15,0.778	15,0.732	15,0.761	15,0.755	15,0.762	15,0.756
4225	20,0.768	20,0.701	15,0.783	15,0.773	15,0.776	15,0.730	15,0.761	16,0.770	15,0.748	15,0.772

Table 15.11: Number of iterations and average reduction factors for p-Minres, Q_2-Q_1 , rectangular mesh, L-shaped island, MG.

$N \setminus m$	10^0	10^1	10^2	10^3	10^4	10^5	10^6	10^7	10^8	10^9
outer-solve										
659	12,0.377	16,0.478	27,0.617	67,0.717	97,0.817	*,0.976	*,0.969	*,0.980	*,0.988	*,0.989
2467	13,0.316	17,0.431	17,0.452	20,0.546	80,0.836	*,0.951	*,0.965	*,0.962	*,0.976	*,0.992
9539	18,0.525	24,0.575	25,0.607	29,0.657	87,0.887	*,0.981	*,0.978	*,0.987	*,0.988	*,0.998
37507	18,0.491	27,0.667	27,0.649	49,0.778	50,0.793	*,0.962	*,0.995	*,0.993	*,0.998	*,0.985
inner-solve										
81	6,0.497	7,0.625	7,0.655	7,0.666	7,0.649	7,0.659	7,0.659	8,0.669	8,0.670	8,0.671
289	8,0.699	9,0.703	9,0.713	9,0.720	9,0.715	9,0.717	9,0.713	10,0.741	10,0.745	10,0.745
1089	9,0.747	11,0.752	11,0.744	11,0.749	11,0.750	11,0.760	11,0.759	12,0.765	12,0.769	12,0.770
4225	12,0.795	13,0.801	13,0.813	13,0.810	13,0.811	13,0.801	13,0.803	14,0.807	14,0.818	14,0.819

Table 15.12: Number of iterations and average reduction factors for p-Minres, Q_2-Q_1 , rectangular mesh, L-shaped island AGKS.

$N \setminus m$	10^0	10^1	10^2	10^3	10^4	10^5	10^6	10^7	10^8	10^9
outer-solve										
659	39,0.746	33,0.694	32,0.697	32,0.677	32,0.706	32,0.696	32,0.689	34,0.718	34,0.748	32,0.819
2467	54,0.816	41,0.731	24,0.752	20,0.656	18,0.556	18,0.555	20,0.585	21,0.595	23,0.606	22,0.760
9539	60,0.845	51,0.760	31,0.687	23,0.591	21,0.492	20,0.591	22,0.583	23,0.577	24,0.578	23,0.608
37507	82,0.871	64,0.476	35,0.509	27,0.508	23,0.503	21,0.502	23,0.500	22,0.499	23,0.500	21,0.525
inner-solve										
81	20,0.797	20,0.703	6,0.588	5,0.577	6,0.581	6,0.532	6,0.575	6,0.553	6,0.569	6,0.565
289	20,0.763	20,0.694	6,0.582	6,0.576	6,0.584	6,0.536	6,0.569	6,0.565	6,0.574	6,0.549
1089	20,0.773	20,0.714	6,0.583	6,0.577	6,0.579	6,0.535	6,0.563	6,0.667	6,0.565	6,0.568
4225	20,0.768	20,0.701	6,0.585	6,0.576	6,0.578	6,0.532	6,0.560	6,0.561	6,0.554	6,0.561

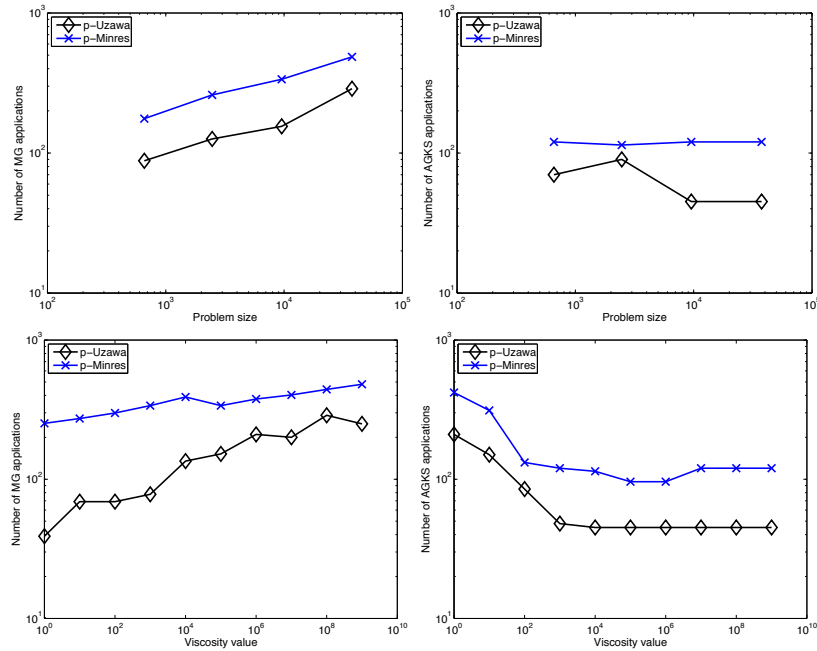


Fig. 15.3: The plot of the number of (top-left) MG applications versus problem size for fixed viscosity value $m = 10^8$, (bottom-left) MG applications versus viscosity value for fixed level = 4 (top-right) AGKS applications vs problem size for fixed viscosity value $m = 10^8$, (bottom-right) AGKS applications versus viscosity value for fixed level = 4.

References

1. Aksoylu, B., Bond, S. & Holst, M. An odyssey into local refinement and multilevel preconditioning III: Implementation and numerical experiments. *SIAM J. Sci. Comput.*, **25**, 478–498, 2003.
2. Aksoylu, B., Graham, I. G., Klie, H. & Scheichl, R. Towards a rigorously justified algebraic preconditioner for high-contrast diffusion problems. *Comput. Vis. Sci.*, **11**, 319–331, 2008.
3. Aksoylu, B. & Beyer, H. R. On the characterization of the asymptotic cases of the diffusion equation with rough coefficients and applications to preconditioning. *Numer. Funct. Anal. Optim.*, **30**, 405–420, 2009.
4. Aksoylu, B. & Beyer, H. R. Results on the diffusion equation with rough coefficients. *SIAM J. Math. Anal.*, **42**, 406–426, 2010.
5. Aksoylu, B. & Klie, H. A family of physics-based preconditioners for solving elliptic equations on highly heterogeneous media. *Appl. Num. Math.*, **59**, 1159–1186, 2009.
6. Aksoylu, B. & Yeter, Z. Robust multigrid preconditioners for cell-centered finite volume discretization of the high-contrast diffusion equation. *Comput. Vis. Sci.*, **13**, 229–245, 2010.
7. Aksoylu, B. & Yeter, Z. Robust multigrid preconditioners for the high-contrast biharmonic plate equation. *Numer. Linear Algeb. Appl.*, **18**, 733–750, 2011.
8. Axelsson, O. *Iterative solution methods*. Cambridge: Cambridge University Press, pp. xiv+654, 1994.

9. Bakhvalov, N. S., Knyazev, A. V. & Parashkevov, R. R. An efficient iterative method for Stokes and Lamé equations for nearly incompressible media with highly discontinuous coefficients. Tech. Report, 1997.
10. Bakhvalov, N. S., Knyazev, A. V. & Parashkevov, R. R. Extension theorems for Stokes and Lamé equations for nearly incompressible media and their applications to numerical solution of problems with highly discontinuous coefficients. *Numer. Linear Algebra Appl.*, **9**, 115–139, 2002.
11. Bank, R. E., Welfert, B. D. & Yserentant, H. A class of iterative methods for solving mixed finite element equations. *Numerische Mathematik*, **56**, 645–666, 1990.
12. Bank, R. E. & Welfert, B. D. A posteriori error estimates for the Stokes equations: a comparison. *Comput. Methods Appl. Mech. Eng.*, **82**, 323–340, 1990.
13. Benzi, M., Golub, G. H. & Liesen, J. Numerical solution of saddle point problems. *Acta Numerica*, **14**, 1–137, 2005.
14. Benzi, M. & Wathen, A. J. Some preconditioning techniques for saddle point problems. *Model Order Reduction: Theory, Research Aspects and Applications* (W. Schilders, H. A. van der Vorst & J. Rommes eds). Mathematics in Industry. Springer-Verlag, pp. 195–211, 2008.
15. Bramble, A., Pasciak, J. & Vassilev, A. Analysis of the inexact Uzawa algorithm for saddle point problems. *SIAM Journal on Numerical Analysis*, 1997.
16. Brezzi, F. & Fortin, M. *Mixed and hybrid finite element methods*. Springer-Verlag, 1991.
17. Elman, H., Howle, V. E., Shadid, J., Shuttleworth, R. & Tuminaro, R. Block preconditioners based on approximate commutators. *SIAM Journal on Scientific Computing*, **27**, 1651–1668, 2006.
18. Elman, H. C. Preconditioning for the steady-state Navier Stokes equations with low viscosity. *SIAM J. Sci. Comput.*, **20**, 1299–1316, 1999.
19. Elman, H. C., Howle, V. E., Shadid, J. N. & Tuminaro, R. S. a parallel block multi-level preconditioner for the 3d incompressible Navier-Stokes equations. *Journal of Computational Physics*, **187**, 504–523, 2003.
20. Elman, H. C., Silvester, D. J. & Wathen, A. J. *Finite elements and fast iterative solvers: with applications in incompressible fluid dynamics*. Numerical Mathematics and Scientific Computation. New York: Oxford University Press, pp. xiv+400, 2005.
21. Elman, H. C., Ramage, A. & Silvester, D. J. Algorithm 866: IFISS, a Matlab toolbox for modelling incompressible flow. *ACM Transactions on Mathematical Software*, **33**, 14. Article 14, 18 pages, 2007.
22. Elman, H. & Golub, G. Inexact and preconditioned Uzawa algorithms for saddle point problems. *SIAM Journal on Numerical Analysis*, 1994.
23. Elman, H. & Silvester, D. Fast nonsymmetric iterations and preconditioning for Navier-Stokes equations. *SIAM J. Sci. Comput.*, **17**, 33–46, 1996.
24. Fortin, M. Some iterative methods for incompressible flow problems. *Comput. Phys. Comm.*, **53**, 393–399, 1989.
25. Fortin, M. & Glowinski, R. *Augmented Lagrangian Methods: Application to the numerical solution of boundary value problems*. North-Holland, Amsterdam, 1983.
26. Furuichi, M., May, D. A. & Tackley, P. J. Development of a Stokes flow solver robust to large viscosity jumps using a Schur complement approach with mixed precision arithmetic. *Journal of Computational Physics*, **230**, 8835–8851, 2011.
27. Furuichi, M. Numerical modeling of three dimensional self-gravitating Stokes flow problem with free surface. *Procedia Computer Science*, **4**, 1506–1515, 2011.
28. Glowinski, R. *Numerical methods for nonlinear variational problems*. New York: Springer-Verlag, 1984.
29. Grinevich, P. P. & Olshanskii, M. A. An iterative method for the Stokes-type problem with variable viscosity. *SIAM J. Sci. Comput.*, **31**, 3959–3978, 2009.
30. K. J. Arrow, L. H. & Uzawa, H. *Studies in linear and non-linear programming*. Stanford, CA: Stanford University Press, 1958.
31. Kay, D., Loghin, D. & Wathen, A. Preconditioner for the steady-state Navier-Stokes equations. *SIAM Journal on Scientific Computing*, **24**, 237–256, 2002.

32. Kobelkov, G. M. & Olshanskii, M. A. Effective preconditioning of uzawa type schemes for a generalized Stokes problem. *Numerische Mathematik*, **86**, 443–470, 2000. 10.1007/s002110000160.
33. Larin, M. & Reusken, A. A comparative study of efficient iterative solvers for generalized Stokes equations. *Numerical Linear Algebra with Applications*, 2007.
34. May, D. A. & Moresi, L. Preconditioned iterative methods for Stokes flow problems arising in computational geodynamics. *Physics of the Earth and Planetary Interiors*, **171**, 33–47, 2008.
35. Moresi, L. N. & Solomatov, V. S. Numerical investigation of 2D convection with extremely large viscosity variations. *Physics of Fluids*, **7**, 2154–2162, 1995.
36. Olshanskii, M. A. & Reusken, A. A Stokes interface problem: stability, finite element analysis and a robust solver. *European congress on computational methods in applied sciences and engineering*, 2004.
37. Olshanskii, M. A. & Reusken, A. Analysis of a Stokes interface problem. *Numerische Mathematik*, **103**, 129–149, 2006.
38. Paige, C. & Saunders, M. A. Solution of sparse indefinite systems of linear equations. *SIAM J. Numer. Anal.*, **12**, 617–629, 1975.
39. Peters, J., Reichelt, V. & Reusken, A. Fast iterative solvers for discrete Stokes equations. *SIAM Journal on Scientific Computing*, **27**, 646–666, 2005.
40. Rusten, T. & Winther, R. A Preconditioned Iterative Method for Saddle Point Problems. *SIAM Journal on Matrix Analysis and Applications*, **13**, 887, 1992.
41. Silvester, D., Elman, H. & Ramage, A. Incompressible Flow and Iterative Solver Software (IFISS) version 3.1, 2011. <http://www.manchester.ac.uk/ifiss/>.
42. Silvester, D. & Wathen, A. Fast iterative solution of stabilised Stokes systems part II: using general block preconditioners. *SIAM Journal on Numerical Analysis*, **31**, 1352–1367, 1994.
43. Stoll, M. & Wathen, A. The Bramble-Pasciak⁺ preconditioner for saddle point problems. *Technical Report*. Oxford, UK: Oxford University Computing Laboratory, Technical report, Report no. 07/13, 2007.
44. ur Rehman, M., Geenen, T., Vuik, C., Segal, G. & MacLachlan, S. On iterative methods for the incompressible Stokes problem. *International Journal for Numerical methods in fluids*, 2010.
45. Wathen, A. & Silvester, D. Fast iterative solution of stabilised Stokes systems. part I: Using simple diagonal preconditioners. *SIAM Journal on Numerical Analysis*, **30**, 630–649, 1993.
46. Zulehner, W. Analysis of iterative methods for saddle point problems: a unified approach. *Math. Comp.*, **71**, 479–505, 2002.